Analyst

Accepted Manuscript

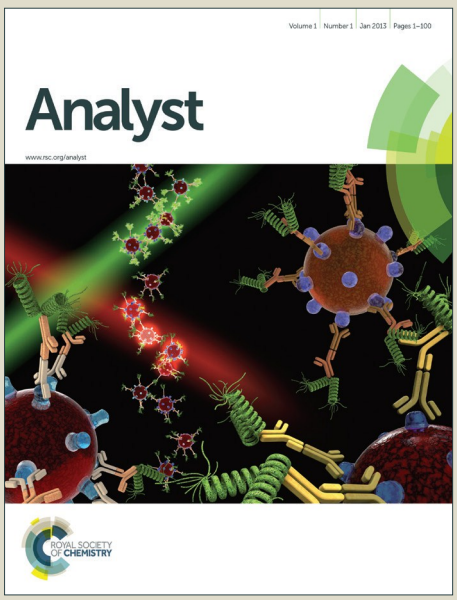

This is an *Accepted Manuscript*, which has been through the Royal Society of Chemistry peer review process and has been accepted for publication.

Accepted Manuscripts are published online shortly after acceptance, before technical editing, formatting and proof reading. Using this free service, authors can make their results available to the community, in citable form, before we publish the edited article. We will replace this *Accepted Manuscript* with the edited and formatted *Advance Article* as soon as it is available.

You can find more information about *Accepted Manuscripts* in the Information for Authors.

Please note that technical editing may introduce minor changes to the text and/or graphics, which may alter content. The journal's standard Terms & Conditions and the Ethical guidelines still apply. In no event shall the Royal Society of Chemistry be held responsible for any errors or omissions in this *Accepted Manuscript* or any consequences arising from the use of any information it contains.

ROYAL SOCIETY OF CHEMISTRY

www.rsc.org/analyst

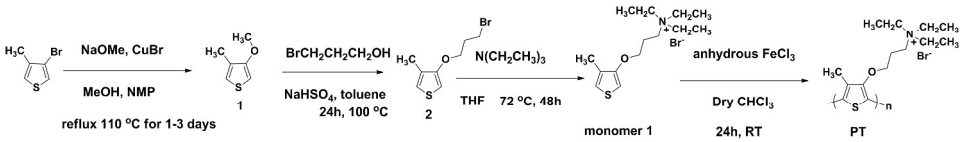

Scheme 1: Synthesis of PT
386x83mm (300 x 300 DPI)

Analyst Accepted Manuscript

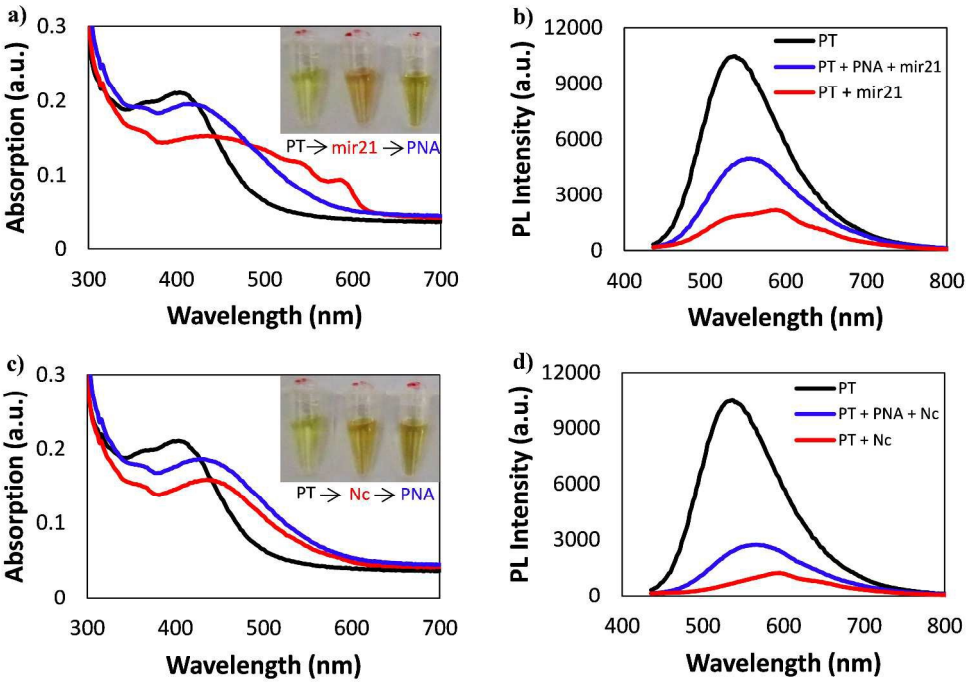

Figure 1: (a,b) Absorption and emission spectra with images (inset Fig. 1a) of PT with subsequent addition of mir21 followed by PNA; (c,d) Absorption and emission spectra with images (inset Fig. 1c) of PT with subsequent addition of Nc sequence followed by PNA
361x258mm (300 x 300 DPI)

Analyst Accepted Manuscript

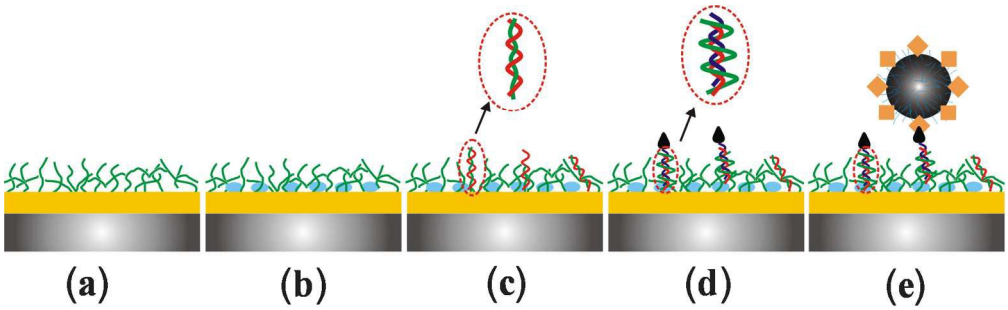

Figure 2: Schematic illustration of the mir21 assay on QCM crystals. Quartz crystal is sequentially exposed to (a) PT, (b) BSA for gold substrate passivation, (c) RNA and duplex formation, (d) b-PNA and triplex formation and (e) ANP for signal amplification
164x51mm (300 x 300 DPI)

Analyst Accepted Manuscript

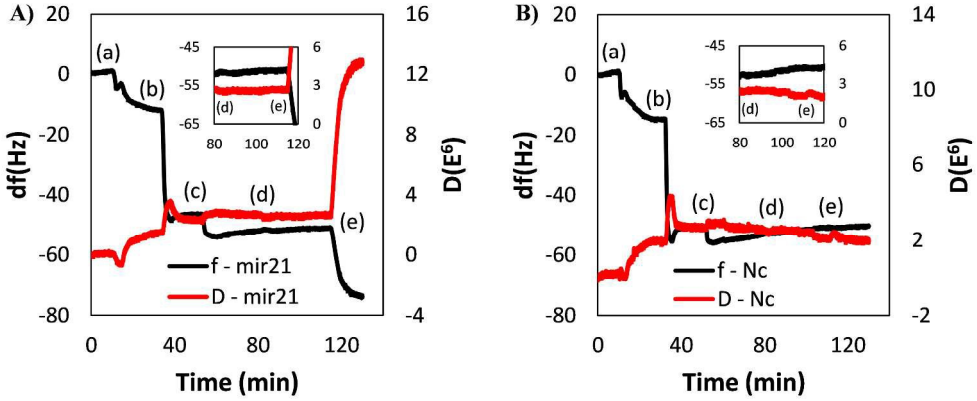

Figure 3: QCM kinetic measurements: Frequency (df) and energy dissipation (D) at the third overtone for (A) mir21 and (B) Nc sequence illustrating responses after the injection of (a) PT, (b) BSA, (c) 10 μM mir21/Nc sequence, (d) b-PNA, and (e) 0.1 mg/ml ANP
358x162mm (300 x 300 DPI)

Analyst Accepted Manuscript

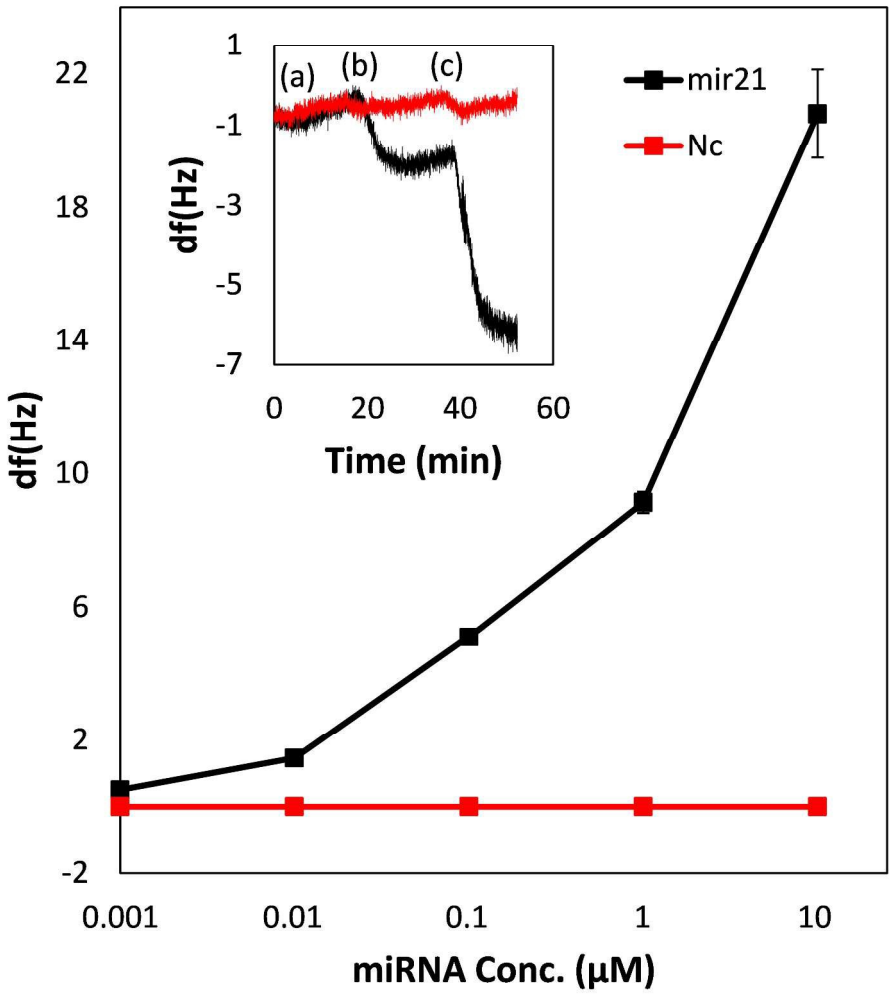

Figure 4: Concentration dependent responses for mir21 and Nc sequence (n=3). Inset: QCM kinetic measurement for mir21 and Nc sequence isolated from plasma (a) b-PNA, (b) 0.1 mg/ml ANP, and (c) 0.5 mg/ml ANP
250x270mm (300 x 300 DPI)

Analyst Accepted Manuscript

Polythiophene derivative on quartz resonators for miRNA capture and assay

Al. Palaniappan [a,b,*], *Jamal Ahmed Cheema* [a,b], *Deepa Rajwar* [a,b], *Gopal Ammanath* [a,b,c], *Liu Xiaohu* [a,b], *Lim Seng Koon* [a,b], *Wang Yi* [a,b], *Umit Hakan Yildiz* [d,e], *Bo Liedberg* [a,b,*]

[a] *School of Materials Science and Engineering, Nanyang Technological University, Singapore 639798*

[b] *Center for Biomimetic Sensor Science, 50 Nanyang Drive, Singapore 637553*

[c] *Nanyang Institute of Technology in Health and Medicine, Interdisciplinary Graduate School, Nanyang Technological University, Singapore 637553*

[d] *Department of Chemistry, Izmir Institute of Technology, 35430, Urla, Izmir/Turkey*

[e] *Stanford University School of Medicine, Palo Alto, California 94304, United States.*

Abstract:

A novel approach for miRNA assay using a cationic polythiophene derivative, poly[3-(3'-N,N,N-triethylamino-1'-propyloxy)-4-methyl-2,5-thiophene hydrobromide] (PT), immobilized on quartz resonator is proposed. Cationic PT enables capturing of all RNA sequences in the sample matrix via electrostatic interactions, resulting in formation of PT-RNA duplex structures on quartz resonators. Biotinylated peptide nuclide acid (b-PNA) sequences are subsequently utilized for the RNA assay, upon monitoring PT-RNA-b-PNA triplex formation. Signal amplification is achieved by anchoring avidin coated nanoparticles to b-PNA in order to yield responses at clinically relevant concentration regimes. Unlike conventional nucleic acid assay methodologies that usually quantify a specific sequence of RNA, the proposed approach enables assay of any RNA sequence in sample matrix upon hybridization with a PNA sequence complementary to the RNA of interest. As an illustration, successful detection of mir21, (miRNA sequence associated with lung cancer) is demonstrated with a limit of detection of 400 pM. Furthermore, precise quantification of mir21 in plasma samples is demonstrated without requiring PCR and sophisticated instrumentation.

Analyst Accepted Manuscript

*Corresponding authors at: Center for Biomimetic Sensor Science, Nanyang Technological University, 50 Nanyang Drive, Singapore 637553.

Tel: +65 6513 7352; Fax: +65 67909081.

E-mail addresses: alps@ntu.edu.sg; bliedberg@ntu.edu.sg

Keywords: Quartz resonator, polythiophene, miRNA, nucleic acid assay

Introduction

Over the past few years, optical properties of conjugated polyelectrolytes (CPEs) have been exploited for applications in nucleic acid assays.[1-9] The assays are based on changes in the optical properties of CPEs that are attributed to the polymer backbone conformation. Upon interaction with nucleic acids, positively charged CPEs form a complex and exhibit changes in colorimetric and fluorometric signals that are enhanced by collective response. Recent studies reveal that optical property changes could even facilitate naked eye detection of nucleic acids.[7-12] However, solution based methodologies often encounter difficulties due to uncontrolled complexation and therefore limiting the selectivity of nucleic acid assay.[13] Moreover, most of the approaches do not yield quantitative analysis without inclusion of sophisticated optical characterization techniques. Optical methods further have limitations to perform quantitative nucleic acid assay in complex samples, for instance, serum. Furthermore, there is a need for a "mix-and-measure" type assay to detect fragile gene fragments as well as microRNA (miRNA) sequences. Therefore, spirited by the recent advances in programmable complex formation upon impregnation of CPEs on paper based solid substrates,[14] we have attempted to utilize a polythiophene derivative which is a cationic CPE, for the first time, as responsive layers on a resonator platform such as quartz crystal microbalance (QCM) for specific and quantitative analysis of miRNA. In this report, cationic polythiophene derivative, poly[3-(3'-*N*,*N*,*N*-triethylamino-1'-propyloxy)-4-methyl-2,5-thiophene hydrobromide] (PT) are immobilized on QCM surface for capturing miRNA via electrostatic interactions.

Cationic PTs are utilized for maximizing the interaction with negatively charged nucleic acids.[8-9] They freely form hydrogels with significant swelling at physiological pH facilitating full capture of miRNA.[15] As reported previously, PT complexes with miRNA via electrostatic interactions yielding a duplex structure.[14,16] PT

Analyst Accepted Manuscript

therefore captures target miRNA and other interfering miRNA in complex samples. Triplex formation or specific detection is achieved upon injection of a PNA sequence complementary to the target miRNA. mir21, a miRNA sequence associated with lung cancer, is utilized in the study for validation of the proposed approach.

Several assay formats based on QCM have been reported, usually involving a recognition molecule immobilized on the QCM crystal surface that can specifically bind a target analyte.[17-19] As for nucleic acid assay, PNA/DNA probes are usually immobilized on QCM surface for detection of a particular DNA/RNA sequence of interest. Though sub-pM detection sensitivities have been reported based on QCM[18-19], most of the reports possess the limitation of quantifying a specific sequence of RNA in the sample matrix. Unlike conventional nucleic acid probes that are immobilized on QCM surface, PT, proposed in this study, enables capturing all miRNA in a sample matrix, providing a unique possibility of detecting any miRNA sequence upon injection of a peptide nucleic acid (PNA) sequence complementary to the miRNA of interest. Avidin coated nanoparticles (ANP) are subsequently utilized for signal amplification and to yield responses at clinically relevant concentration regimes. Avidin functionalized nanoparticles selectively bind to the biotin anchored to PNA. ANPs serve as mass enhancers amplifying the PNA hybridization signal. QCM frequency shift responses are then directly correlated to miRNA concentration, thereby eliminating the need for PCR upon miRNA isolation.

Experimental

All the chemicals for PT synthesis were purchased from Sigma–Aldrich and used without further purification. Deionized (DI) MilliQ water (resistivity of 18 MΩ-cm) was used for buffer preparation and PT synthesis. Precursors 1 and 2 were synthesized according to previous reports.[20] Quaternization of precursor 2 with triethylamine yielded monomer 1. PT was subsequently synthesized by oxidative polymerization of monomer 1 (Scheme 1). Structure of the precursors and monomers were confirmed by NMR spectroscopy. Number averaged molecular weight of synthesized PT is estimated to be between 6 and 10 kDa.[21] Similarly, PT with varying pendant groups was synthesized in order to investigate/optimize their interaction with miRNA (Fig. S1). Perkin Elmer lambda 35 UV-vis spectrometer, Infinite M200Pro tecan plate reader and Thermo Scientific

Analyst Accepted Manuscript

Nanodrop 2000c Spectrophotometer were used for optical characterization of synthesized PT, prior to applying the polymer in the QCM based assay.

5 MHz AT-cut piezoelectric quartz crystals coated with gold were obtained from Q-Sense, Sweden. QCM crystals were cleaned before use by first treating them with ozone for 10 min followed by sonication in 99 % ethanol for 5 min. Crystals were then rinsed with ethanol followed by DI water and blown dry with N_2. The cleaned crystals were mounted in the microfluidic chamber of the Q-Sense instrument. Real time QCM measurements were carried out using Q-Sense E4. Upon attaining stable resonant frequency, 250 µL of varying concentrations of PT was injected (at a flow rate of 50 µL/min) into the QCM chamber. An optimized concentration of 0.1 mg/ml based on polymer loading was chosen for the assay (Fig. S2) to form a layer of ~ 2.8 nm thickness (Fig. S3). PBS with 0.002 % tween (PBST) was used as running buffer solution and for PNA/miRNA dilutions.

The following miRNA and PNA sequences were purchased from IDT and Panagene, respectively.

mir21: 5'- UAG CUU AUC AGA CUG AUG UUG A - 3'

Non-complementary sequence (Nc): 5'- AUG CAU GCA UGC AUG CAU GCA A - 3'

Biotinylated PNA sequence (b-PNA): Biotin - OO – 5' TCA ACA TCA GTC TGA TAA GCT A 3', where O represents a glycol spacer.

miRNA stock solutions of 100 µM were prepared with RNase free DI water and stored at -20 °C. For miRNA assay, PT addition was followed by injections of 250 µL of bovine serum albumin (BSA, 5 mg/ml), 250 µL of miRNA (at varying concentrations), 250 µL of b-PNA and 0.1 mg/ml ANP. ANP, purchased from Chemicell GmbH, Germany, comprises of a magnetite core covered in a starch matrix and functionalized with avidin. The particles are of ~100 nm in size and suspended in PBS with 0.05% sodium azide buffer. Human plasma was purchased from GeneTex, Taiwan for spiking experiments, upon isolation of mir21 using Macherey-Nagel's Nucleospin miRNA extraction kit.

Results and Discussion

Optical Characterization of PT

Analyst Accepted Manuscript

In order to understand and validate PT as responsive layer upon interaction with mir21, absorption and fluorescence spectra of 150 μM of PT in the presence and absence of 10 μM miRNA were recorded at room temperature. The UV–Vis absorption and emission maxima in DI water solution of PT have been observed at 403 nm and 537 nm, respectively. These peaks are due to the random coil morphology of PT backbone and are in agreement with previous reports.[14,22-24] Figures 1a and 1c show red shifts from the main absorption peak (403 nm) upon addition of 30 μL of 10 μM mir21 and the Nc sequence (red curves), respectively. For the mir21, redistribution of absorption spectrum with main absorption peak at 442 nm, and two vibronic peaks at 541 nm and 589 nm was observed, whereas a single broad absorption curve with maxima at 439 nm was observed for Nc. This difference in the absorption peak is possibly because of the difference in the interaction mode of PT with mir21 and Nc, due to the very sensitive nature of PT backbone (changing conformation from nonplanar to planar) towards different nucleotides. As reported previously, the red shift is attributed to PT-miRNA duplex formation governed by electrostatic interactions between PT and miRNA sequences.[14] Figure 1a shows that a prominent blue shift of the main absorption peak, ~30 nm, was observed for mir21 compared to the Nc sequence (Fig. 1c) upon addition of PNA sequence complementary to mir21 (blue curve).

The fluorescence emission spectra show a significant quenching of PT fluorescence upon exposure to mir21 and Nc sequences. As observed from Fig. 1b and 1d, recovery of the fluorescence upon addition of PNA is significantly higher for mir21 in comparison to the Nc sequence, due to the change from planar to a non-planar "random" backbone of PT in PT-PNA-mir21 triplex construct. The optical images of vials containing PT with mir21 and with Nc sequences (insets in Fig. 1a and 1c, respectively) indicate similar colorimetric response for the two sequences. However, recovery in colorimetric response is more evident for mir21 upon addition of complementary PNA sequence, in agreement with UV-Vis spectra (the red and blue curves in Fig. 1a and 1c). Figure 1 ascertains that the optical shifts are consistent with duplex/triplex formation and that the synthesized PT could be utilized as optically responsive layers. Herein, we explore the potential of immobilizing PT on QCM surfaces for specific and quantitative analysis of miRNA.

QCM assay

Analyst Accepted Manuscript

The proposed assay (Fig. 2), involves sequential injection of synthesized PT and BSA in QCM chamber, followed by miRNA and a complementary sequence of b-PNA for hybridization with target miRNA sequence; ANP are subsequently utilized for amplified detection of miRNA. PT was injected simultaneously in two chambers mounted with cleaned QCM crystals. Upon injection of PT, a two-step frequency response (Fig. 3 (a) to (b)) was observed due to changes in morphology of PT upon buffer exchange between DI water and PBST, in agreement with previous reports.[24] Surface mass coverage of the PT as revealed by SPR was estimated to be ~ 158 ng/cm^2; corresponding to a thickness of ~2.8 nm and density of ~1.2×10^{13} molecule/cm^2, further indicating PT immobilization on QCM surface (see Fig. S3 for experimental details). 5 mg/ml BSA in PBST was then injected for substrate passivation in order to minimize physisorption) of ANP and other interfering species present in complex matrices on Au surfaces (b, if any. 10 µM of mir21 and 10 µM of Nc sequences were then injected in chamber 1 and 2, respectively. Identical resonance frequency shifts of ~5 Hz (c) were obtained for both mir21 and Nc sequences indicating that synthesized PT captures both Nc and mir21 sequences. 10 µM b-PNA complementary to mir21 was subsequently injected in both channels, followed by injection of ANP. Although no obvious frequency or dissipation shifts (0.5 Hz and 0.27E^6, respectively) were noticed upon b-PNA hybridization with mir21 (d), significant frequency and dissipation shifts (20 Hz and 10E^6, respectively) were observed upon injection of 0.1 mg/ml ANP (e). PNA-mir21-PT triplex formation is therefore ascertained as only a negligible shift was recorded for the Nc-PT duplex, indicating successful capture of miRNA by PT immobilized on Au surface and selective recognition of the mir21-PT duplex by b-PNA. As shown in Fig. 3, approximately 40-fold signal amplification, a shift of 20 Hz upon ANP addition compared to ~0.5 Hz for mir21, was achieved by injection of ANP.

Selective detection of mir21

Concentration dependent responses (Fig. 4) reveal that frequency shifts were observed only when mir21 is captured by PT immobilized on QCM surface. Almost negligible responses were obtained for all test concentrations of Nc RNA (curve Nc) indicating minimum interaction and binding between Nc and b-PNA (complementary to mir21)/ANP. A frequency shift of ~ 5 Hz was obtained for 100 nM of mir21 compared to ~

Analyst Accepted Manuscript

0.5 Hz for 100 nM of Nc sequence, illustrating that incorporation of capture and amplification methodologies enables selective detection of miRNA. Quantification of miRNA is subsequently achieved by correlating frequency responses with mir21 concentrations. As observed from Fig. 4, frequency responses were obtained for 1 nM to 10 μM mir21, with a limit of detection of 400 pM, calculated using $3\sigma/S$,[25] where σ is the standard deviation and S is the slope of concentration response, derived at lower linear response range [between 1 nM and 10 nM, Fig. 4]. Repeatable frequency responses for all test concentrations of mir21 and Nc (n=3) were obtained indicating homogeneity in PT adsorption on QCM surfaces. The proposed methodology therefore illustrates the potential for analysis of complex samples containing miRNA in the clinically relevant nM concentration ranges.[21,26,27]

mir21 assay in plasma

The mir21 assay was then carried out using plasma for demonstrating the applicability of the proposed approach for complex matrices. Plasma samples were spiked with 1 μM of mir21 to mimic clinical samples. Commercially available extraction kits were then used for miRNA isolation, in order to minimize potential interference associated with physisorption of plasma components. mir21 isolation was carried out adopting the standard protocol shown in Fig. S4. For control measurements, same protocol was adopted for plasma samples spiked with 1 μM of Nc sequence. UV-Vis analysis was carried out at each step of isolation process to confirm mir21 and Nc RNA extraction from plasma samples (Fig. S5). Inset in Fig. 4 shows a negligible shift for plasma sample spiked with mir21 and Nc sequence upon injection of b-PNA (a). Following the injection of 0.1 mg/ml ANP, a frequency shift of ~ 2 Hz was observed for mir21 spiked plasma samples (b) compared to a negligible shift for plasma samples spiked with the Nc sequence. Experimental results indicate amplification enhancement could be achieved upon increasing the concentration of ANP. A further increase in frequency response ~ 4 Hz (c) was observed upon injection of 0.5 mg/ml ANP to the plasma sample spiked with mir21. However, as observed from Fig. 4 inset, increasing concentration of ANP resulted in higher signal to noise ratios. Further studies will therefore focus on optimization of assay and amplification protocols, emphasizing on sensitivity and selectivity enhancement, for instance, tailoring the terminal groups of PT for maximizing RNA capture and

Analyst Accepted Manuscript

assay. Nevertheless, the proposed capture methodology enabled quantification of mir21 in plasma samples without requiring PCR and sophisticated instrumentation.

Conclusion

A cationic polythiophene derivative has been deposited on quartz resonator such as QCM for mir21 assay using b-PNA and ANP amplification. The proposed methodology provides an approach to capture all miRNA sequences in the sample as compared to conventional assays that quantify a specific sequence of RNA. Successful detection of mir21 was carried out at clinically relevant concentrations with a limit of detection of 400 pM. Since QCM offers portability, the proposed methodology is feasible for development of point of care devices. Furthermore, assay of other RNA sequences of interest could be carried out upon utilization of appropriate complementary PNA sequences.

Acknowledgement

The authors wish to acknowledge the research grant [Academic Research Fund (AcRF) Tier 1 MOE] from Nanyang Technological University, Singapore, to conduct this study.

Analyst Accepted Manuscript

References:

1) B. Liu and G.C. Bazan, *Chem. Mater.*, 2004, **16**, 4467−4476.

2) A.C. Carreon, W.L. Santos, J.B. Matson and R.C. So, *Polym. Chem.,* 2014, **5,** 314-317.

3) W. Zheng and L. He, *Biomater. Sci.*, 2014, **2**, 1471-1479.

4) W. Zheng and L. He, *J. Am. Chem. Soc.*, 2009, **131**, 3432-3433.

5) B. Fang, S. Jiao, M. Li, Y. Qu and X. Jiang, *Biosens. Bioelectron.*, 2008, **23**, 1175-1179.

6) K.P.R. Nilsson and O. Inganäs, *Nat. Mater.*, 2003, **2**, 419-424.

7) H.A. Ho, A. Najari and M. Leclerc, *Acc. Chem. Res.*, 2008, **41**, 168−178.

8) H.A. Ho, M. Boissinot, M.G. Bergeron, G. Corbeil, K. Dore, D. Boudreau and M. Leclerc, *Angew. Chem. Int. Ed.*, 2002, **41**, 1548-1551.

9) Y. Zhang, Z. Li, Y. Cheng and X. Lv, *Chem. Commun.*, 2009, **22**, 3172-3174.

10) S.W. Thomas, G.D. Joly and T.M. Swager, *Chem. Rev.*, 2007, **107**, 1339−1386.

11) H. Jiang, P. Taranekar, J.R. Reynolds and K.S. Schanze, *Angew. Chem. Int. Ed.*, 2009, **48**, 4300−4316.

12) A. Najari, A.H. Ho, J.F. Gravel, P. Nobert, D. Boudreau and M. Leclerc, *M. Anal. Chem.*, 2006, **78**, 7896-7899.

13) K. Lee, L.K. Povlich and J. Kim, *Analyst*, 2010, **135**, 2179−2189.

14) U.H. Yildiz, A. Palaniappan and B. Liedberg, *Anal. Chem.*, 2013, **85**, 820−824.

15) P. Åsberg, P. Björk, F. Höök and O. Inganäs, *Langmuir*, 2005, **21**, 7292-7298.

16) K. Dore, S. Dubus, H.A. Ho, I. Levesque, M. Brunette, G. Corbeil, M. Boissinot, G. Boivin, M.G. Bergeron, D. Boudreau and M. Leclerc, *J. Am. Chem. Soc.*, 2004, **126**, 4240-4244.

17) K.A. Marx, *Biomacromolecules,* 2003, **4**, 1099-1120.

18) J. Wan, X. Liu, Y. Zhang, Q. Gao, H. Qi and C. Zhang, *Sens. Actuators, B*, 2015, **213**, 409-416.

19) Z. Ge, M. Lin, P. Wang, H. Pei, J. Yan, J. Shi, Q. Huang, D. He, C. Fan and X. Zuo, *Anal. Chem.*, 2014, **86**, 2124-2130.

20) C. Li, M. Numata, A.H. Bae, K. Sakurai and S. Shinkai, *J. Am. Chem. Soc.*, 2005, **127**, 4548-4549.

Analyst Accepted Manuscript

21) P.S. Mitchell, R.K. Parkin, E.M. Kroh, B.R. Fritz, S.K. Wyman, E.L. Pogosova-Agadjanyan, A. Peterson, J. Noteboom, K.C. O'Briant, A. Allen, D.W. Lin, N. Urban, C.W. Drescher, B.S. Knudsen, D.L. Stirewalt, R. Gentleman, R.L. Vessella, P.S. Nelson, D.B. Martin and M. Tewari, *Proc. Natl. Acad. Sci. U.S.A.*, 2008, **105**, 10513−10518.

22) Z. Liu, H.L. Wang and M. Cotlet, *Chem. Commun.*, 2014, **50**, 11311-11313.

23) B. Liu and G.C. Bazan, *J. Am. Chem. Soc.*, 2004, **126**, 1942-1943.

24) E. Li, L. Lin, L. Wang, M. Pei, J. Xu and G. Zhang, *Macromol. Chem. Phys.*, 2012, **213**, 887-892.

25) L. Torsi, G.M. Farinola, F. Merinelli, M.C. Tanese, O.H. Omar, L. Valli, F. Babudri, F. Palmisano, P.G. Zambonin and F. Naso, *Nat. Mater.*, 2008, **7**, 412-417.

26) S. Catuogno, C.L. Esposito, C. Quintavalle, L. Cerchia, G. Condorelli and V. Franciscis, *Cancers,* 2011, **3**, 1887−1898.

27) X. Pan, Z. Wang and R. Wang, *Cancer Biol. Ther.*, 2010, **10**, 1224−1232.

Analyst Accepted Manuscript

Figure Captions:

Scheme 1: Synthesis of PT

Figure 1: (a,b) Absorption and emission spectra with images (inset Fig. 1a) of PT with subsequent addition of mir21 followed by PNA; (c,d) Absorption and emission spectra with images (inset Fig. 1c) of PT with subsequent addition of Nc sequence followed by PNA

Figure 2: Schematic illustration of the mir21 assay on QCM crystals. Quartz crystal is sequentially exposed to (a) PT, (b) BSA for gold substrate passivation, (c) RNA and duplex formation, (d) b-PNA and triplex formation and (e) ANP for signal amplification

Figure 3: QCM kinetic measurements: Frequency (df) and energy dissipation (D) at the third overtone for (A) mir21 and (B) Nc sequence illustrating responses after the injection of (a) PT, (b) BSA, (c) 10 μM mir21/Nc sequence, (d) b-PNA, and (e) 0.1 mg/ml ANP

Figure 4: Concentration dependent responses for mir21 and Nc sequence (n=3). Inset: QCM kinetic measurement for mir21 and Nc sequence isolated from plasma (a) b-PNA, (b) 0.1 mg/ml ANP, and (c) 0.5 mg/ml ANP

Analyst Accepted Manuscript